Experimental Demonstration of Double Emittance Exchange toward Arbitrary Longitudinal Beam Phase-Space Manipulations

Jimin Seok, Gwanghui Ha, John Power, Manoel Conde, Eric Wisniewski, Wanming Liu, Scott Doran, Charles Whiteford, and Moses Chung

Phys. Rev. Lett. **129**, 224801 — Published 23 November 2022

DOI: 10.1103/PhysRevLett.129.224801

First experimental demonstration of double emittance exchange towards arbitrary longitudinal beam phase-space manipulations

Jimin Seok,[1,2] Gwanghui Ha,[2,*] John Power,[2,†] Manoel Conde,[2] Eric Wisniewski,[2]
Wanming Liu,[2] Scott Doran,[2] Charles Whiteford,[2] and Moses Chung[1,‡]

[1]*Intense Beam and Accelerator Laboratory, Department of Physics, Ulsan National Institute of Science and Technology, Ulsan 44919, South Korea*
[2]*Argonne National Laboratory, Lemont, Illinois 60439, USA*
(Dated: October 26, 2022)

Many of the most significant advances in accelerator science have been due to improvements in our ability to manipulate beam phase-space. Despite steady progress in beam phase-space manipulation over the last several decades, future accelerator applications continue to outpace the ability to manipulate the phase-space. This situation is especially pronounced for longitudinal beam phase-space manipulation, and is now getting increased attention. Herein, we report the first experimental demonstration of the double emittance exchange (DEEX) concept, which allows for the control of the longitudinal phase-space using relatively simple transverse manipulation techniques. The DEEX beamline enables extensive longitudinal manipulation, including tunable bunch compression, time–energy correlation control, and nonlinearity correction, in a remarkably flexible manner. The demonstration of this new method opens the door for arbitrary longitudinal beam manipulations capable of responding to the ever increasing demands of future accelerator applications.

Introduction.— The stunning success of the linear accelerator-based light source (i.e., X-ray free electron lasers) in the 2010s was driven by the development of bunch compression and high-brightness sources in the 1990s and 2000s. Continued advances in phase-space manipulation are needed to enable the next generation particle accelerators. This is especially true for longitudinal beam phase-space manipulation, and it have therefore become an increasingly active area of research in modern electron accelerator facilities [1–5]. These methods pursues high-brightness, high-temporal-resolution, controllable bandwidth, etc. It is also getting remarkable attention in the field of future accelerators such as plasma or structure wakefield-based accelerators [6–12] due to the desire for *efficient and sustainable* acceleration. Whereas the beam manipulations in the transverse direction are routinely achieved using magnets, longitudinal beam manipulations often requires specialized beamline configurations (e.g., magnetic bunch compressors [13]), and dedicated radio-frequency (rf) systems (e.g., harmonic rf cavities [14] and de-chirpers [15, 16]). The accelerator field would greatly benefit from a flexible and arbitrary longitudinal beam phase-space manipulation method, capable of responding to the demands of modern and future accelerator science.

We present a new method of longitudinal beam manipulation based on the novel emittance exchange (EEX) concept, which is a potential candidate for realizing flexible and arbitrary longitudinal manipulation. EEX itself is a well-known technique that was proposed for exchanging the longitudinal and horizontal phase-spaces [17–19]. Previous applications have used a single EEX beamline for exploiting the mature methods of transverse manipulation to control the longitudinal phase-space [20–25]. However, the single EEX scheme is known to have several limitations in practical scenarios [26–28] such as a large longitudinal emittance. This results in a large final horizontal emittance which limits horizontal focusing, brightness, and spatial resolution. To maintain low transverse emittance, the idea of adding a second EEX beamline, to exchange the phase spaces once again, was proposed by A. Zholents and M. Zolotorev [28]. In this method, the control of the longitudinal phase-space (LPS) is done after first converting it to a transverse one (see Ref. [29] for further details). Although the method was proposed in 2011, it has not been demonstrated due to concerns over certain limiting effects (e.g. terms higher than second order and collective effects) and the absence of a dedicated experimental facility. A program at Argonne National Laboratory has been aimed at realizing the concept over the last several years [26, 27, 30–32] for the purpose of demonstrating the new concept of flexible LPS manipulation.

In this Letter, we report on the first experimental demonstration of flexible LPS control based on a double EEX (DEEX). This beamline provides three functions for longitudinal bunch manipulation: tunable bunch compression, time–energy correlation (i.e., longitudinal chirp) control, and third-order nonlinearity correction. This method opens the new door for arbitrary and flexible LPS manipulation which can be used to substantially advance future the field of accelerator-based science.

Experimental Setup.— To enable complete emittance exchange, we chose a beamline of two double dogleg-type EEX beamlines [33, 34] rather than the two chicane-type EEX beamlines, as was originally proposed [17, 28]. We designed the middle section (between the two EEX beamlines) to (i) limit the transverse offsets converted from the timing jitter within the linear regimes of the external fields and (ii) use a nonlinear magnet to control the

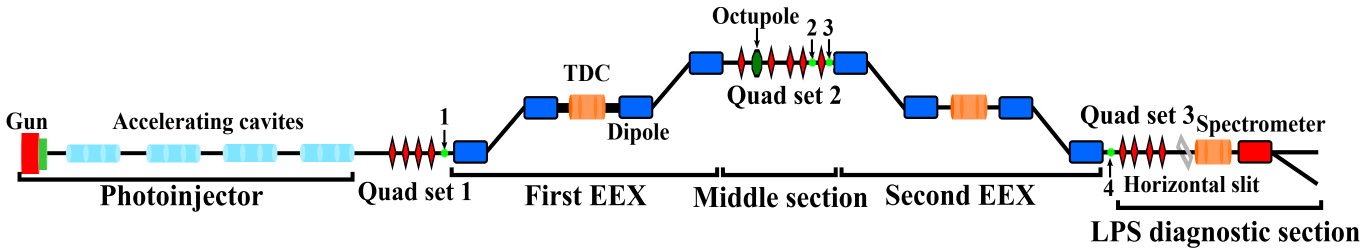

FIG. 1. Experimental beamline configuration. The beamline is composed of a photoinjector, matching quadrupoles (Quad set 1), a DEEX beamline, and an LPS diagnostic section. The photoinjector includes an rf photocathode gun and four accelerating cavities that accelerate the electron beam energy up to 44.5 MeV. The DEEX beamline consists of two EEX beamlines with a middle section for transverse manipulations between them. The LPS diagnostic section follows the second EEX beamline, and it is equipped with four quadrupole magnets (Quad set 3) for transverse focusing, a horizontal slit with a 100-µm opening, a TDC, and a spectrometer. Green dots indicate reference positions 1, 2, 3, and 4 on the experimental beamline.

nonlinearity of the longitudinal time-energy correlation.

A DEEX beamline was installed at the Argonne Wakefield Accelerator (AWA) facility [27, 35]. The experimental beamline consists of a photoinjector, a DEEX beamline, and an LPS measurement section; see Fig. 1. A 300-fs-long laser pulse illuminated a photocathode, and 100 pC and 700 pC electron bunches were generated for each demonstration. Even though the laser pulse length was 300 fs, the bunch length could be elongated at the beam emission and low-energy beam propagation due to space-charge forces. The following accelerating cavities accelerated the bunches to 44.5 MeV. These conditions meant that the space-charge forces in the beam, which can change the beam's behavior, were negligible in the DEEX beamline.

A first set of quadrupole magnets (Quad set 1 in Fig. 1) was used as the DEEX beamline matching quadrupoles. These were followed by a DEEX beamline that consisted of two EEX beamlines and a middle section between them for transverse manipulations. The first EEX beamline exposed the incident longitudinal beam phase-space as a horizontal one into a middle section. A total of five quadrupole magnets (Quad set 2) were located in the middle section for transverse manipulations. Here, the quadrupole magnet's effective length was 0.11 m. Each EEX beamline consisted of four rectangular dipole magnets with a transverse deflecting cavity (TDC) between them. Each of the EEX beamlines had two identical dogleg sections, which bend the beam to the same degree but in opposite directions. The dogleg provided a bending angle of 20° and a dispersion of 0.69 m. The power level applied to the TDC was adjusted to satisfy the exchange condition. The required kick strength (κ) of the TDC was 1.44 m^{-1}, and the rf power applied to the cavity was 2.46 MW. The total length of the DEEX beamline was 12.68 m. Further details can be obtained from Refs. [27, 35, 36].

An LPS diagnostic section was located at the end of the beamline; it consisted of four quadrupoles (Quad set 3), a 100-µm-wide horizontal slit, a TDC, and a 20° bending spectrometer. The Quad set 3 was used to focus the beam transversely at a YAG measurement screen, and the slit was used to transmit a vertical slice of the beam. The TDC then streaked the beam vertically, and the spectrometer bent it horizontally [37]. This projection-based measurement requires a multiplication factor to convert measured data to actual time and energy data.

Experimental Results.— The final root mean square (rms) bunch length (measured at position 4 in Fig. 1) can be expressed in terms of the horizontal rms beam parameters at the entrance of the second EEX beamline (i.e., at position 3) as follows [25]:

$$\sigma_{z,4}^2 = \left\{ R_{51} + R_{52} \left(s_{x,2} - \frac{1}{f_5} \right) \right\}^2 \sigma_{x,3}^2 + \frac{R_{52}^2 \varepsilon_{x,3}^2}{\sigma_{x,3}^2}, \quad (1)$$

where $\sigma_{x,3}$ and $\varepsilon_{x,3}$ denote the horizontal rms beam size and emittance after the last quadrupole in the middle section, respectively. The phase-space slope before the last quadrupole (i.e., at position 2) is given by $s_{x,2} \equiv \sigma_{xx',2}/\sigma_{x,2}^2$. Here, R_{51} and R_{52} are the (5,1) and (5,2) elements of the transfer matrix from position 3 to position 4, and f_5 is the focal length of the last quadrupole. Note that a thin-quadrupole magnet was assumed in Eq. (1) for simplicity; however, all data analyses used a thick-quadrupole magnet (see Ref. [29] for further details). The equation indicates that the final bunch length is a function of the strength of the last quadrupole magnet; thus, the compression is remarkably flexible. Moreover, contrary to conventional magnetic bunch compressors, chirp control is not required for the compression of the bunch.

Figure 2 summarizes the measurement and estimation results. The initial bunch length of 0.36 ± 0.02 mm (red dashed line) was compressed to the minimum final bunch length of 0.08 ± 0.01 mm using the optimized quadrupole setting, which was identified using the transfer matrix of each EEX beamline and the measured beam conditions. We estimated the transfer matrices theoretically using the design parameters; for example, the matrix elements in Eq. (1) were R_{51}=-0.337 and R_{52}=-0.755 m. The beam conditions were measured using the quadrupole

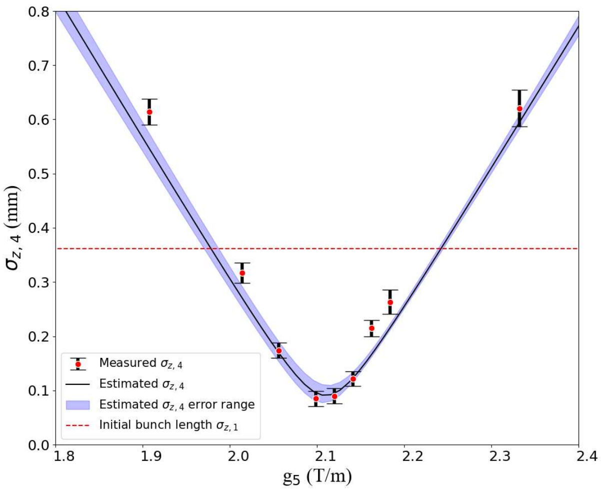

FIG. 2. Tunable bunch compression by DEEX beamline. The last quadrupole magnet in the middle section was scanned during the experiment. The red dots (with associated error bars) represent the measured final bunch lengths ($\sigma_{z,4}$) for each value of the quadrupole gradient (g_5). The black curve indicates the final bunch length, which is estimated using Eq. (1). Because the quadrupole scan results are used to estimate $\varepsilon_{x,3}$ in Eq. (1), the black curve includes a finite error range, which is displayed as the blue shaded area. The red dashed line indicates the bunch length ($\sigma_{z,1}$) at the entrance of the DEEX beamline (position 1).

scan method [38]. The measured beam parameters were $\sigma_{x,3} = 4.29 \pm 0.13$ mm, $s_{x,2} = 1.128 \pm 0.002$ m^{-1}, and $\varepsilon_{x,3} = 0.45 \pm 0.11$ µm. The last quadrupole's gradient (g_5) was varied from 1.91 to 2.33 T/m. We observed both bunch compression and lengthening in a scan of the last quadrupole magnet in the middle section. The measured values of $\sigma_{z,4}$ are consistent with the estimated values.

The minimum bunch length that the DEEX beamline can generate is typically limited by two main factors. The first limiting factor is the initial longitudinal emittance, which becomes the horizontal emittance after the first EEX [$\varepsilon_{x,3}$ in Eq. (1)]. As shown in Eq. (1), the minimum final bunch length is $\frac{R_{52}\varepsilon_{x,3}}{\sigma_{x,3}}$, which is determined by the emittance. In this experiment, the photoinjector provided a relatively large longitudinal emittance (0.45 µm); therefore, the demonstrated compression was limited to a factor of four.

The second limiting factor is the thick-cavity effect. In an ideal EEX beamline, the thickness of the TDC is assumed to be zero. However, a realistic EEX beamline includes the finite length of the TDC; therefore, the initial LPS contributes to the final LPS to some extent [18, 28]. This phenomenon is known as the thick-cavity (or thick-lens) effect. The thick-cavity contributions increase the LPS and bunch length compared with the case of an ideal beamline [19]. Several methods were devised to mitigate or compensate the thick-cavity effect [18, 28, 39]. A commonly used method involves the application of a longitudinal chirp through the rf cavities before the EEX. However, in the case of a DEEX beamline, the thick-cavity effect at the second EEX can be minimized using Quad set 1 before the DEEX beamline. These quadrupoles generate an appropriate longitudinal chirp in the middle section via EEX without any rf chirp control. During the experiment, the Quad set 1 was adjusted to minimize the thick-cavity effect in the second EEX beamline.

Flexible longitudinal chirp control is another unique function of a DEEX beamline that other existing methods cannot provide. This allows to avoid the use of de-chirpers or off-crest acceleration downstream of the bunch compressor. The longitudinal chirp ($\mathcal{C}$) after the DEEX beamline can be written as a function of the final bunch length at position 4 and horizontal slope at position 3 in Fig. 1 [40]:

$$\mathcal{C} = \left(\frac{R_{62}}{2R_{52}} + \frac{B}{2A}\right) + \left(\frac{R_{62}}{2R_{52}} - \frac{B}{2A}\right)\sqrt{1 - \frac{2AR_{52}\varepsilon_{x,3}}{\sigma_{z,4}^2}}, \tag{2}$$

where $A = R_{51} + R_{52}s_{x,3}$ and $B = R_{61} + R_{62}s_{x,3}$. This relationship assumes that the rms beam size at position 3 satisfies the condition

$$\sigma_{x,3}^2 = \frac{\sigma_{z,4}^2 - \sqrt{\sigma_{z,4}^4 - 4A^2R_{52}^2\varepsilon_{x,3}^2}}{2A^2}. \tag{3}$$

Similar to the tunable bunch compression described in Eq. (1), the final longitudinal chirp is controlled by the horizontal slope at the end of the middle section, which can be easily adjusted by quadrupole magnets. Here, two or more quadrupole magnets may be required to control the slope while satisfying Eq. (3). Note that the chirp control range is wide, even in the strong-compression regime ($A \ll 1$). The chirp in this case can be approximated as

$$\mathcal{C} \simeq \frac{R_{62}}{R_{52}} - \frac{R_{52}\varepsilon_{x,3}^2}{\sigma_{z,4}^4}A. \tag{4}$$

However, when the bunch is fully compressed and reaches its minimum, the chirp becomes a fixed number $\frac{R_{62}}{R_{52}}$, as expected from Liouville's theorem.

During the experiment, we used several different combinations of the last two quadrupole magnets in the Quad set 2 so that the chirp was varied while the final bunch length remained constant. Figure 3 shows the measured LPS as well as the corresponding rms bunch length and longitudinal chirp. The LPS is given in terms of the longitudinal position (z) and relative energy deviation (δ). The quadrupole magnets in the middle section were initially set to generate the final beam distribution, as depicted in Fig. 3(a). Subsequently, we increased the

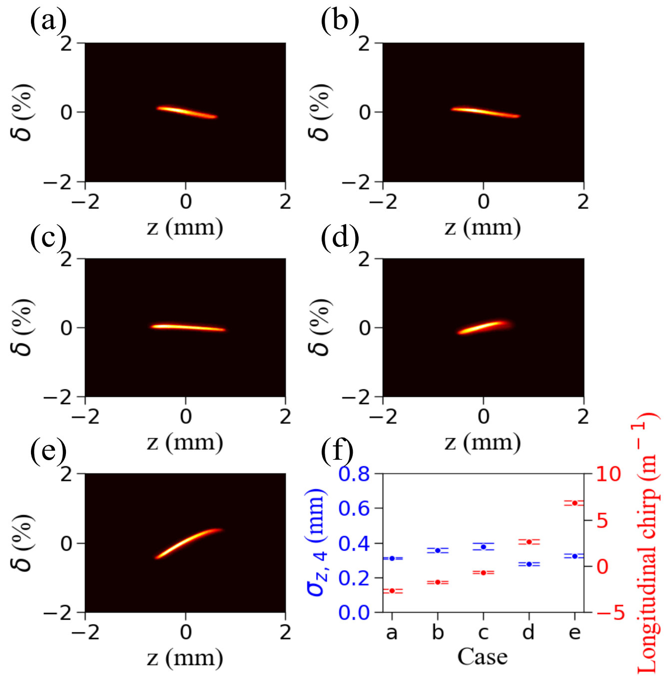

FIG. 3. Longitudinal chirp control by DEEX beamline. (a)–(e) show the measured longitudinal phase spaces with various combinations of the last two quadrupole magnets in the middle section. (f) shows $\sigma_{z,4}$ and the final longitudinal chirps corresponding to each case.

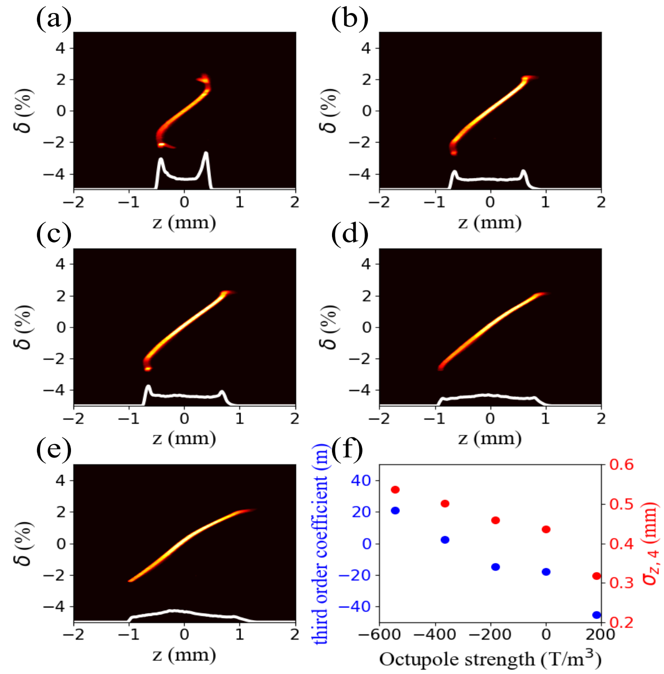

FIG. 4. Third-order correction using an octupole magnet. (a)–(e) show measured longitudinal phase spaces with different octupole magnet strengths. The strengths of the octupole magnet were (182, 0, -182, -364, -546) T/m^3. Each value corresponds to (a)–(e), respectively. (f) shows the third-order coefficient (a_3) of the polynomial fitting and the final bunch length ($\sigma_{z,4}$) for each of the displayed cases.

gradients of the last two quadrupoles. The combinations of the quadrupole magnet strengths were (0.93, 0.94) T/m, (1.87, 0.06) T/m, (3.69, -2.94) T/m, (4.07, -3.45) T/m, and (3.69, -2.51) T/m. Each quadrupole combination corresponds to Figs. 3(a)–(e), respectively. The longitudinal chirp gradually increased from -2.70 m^{-1} to 6.83 m^{-1}, whereas the rms bunch lengths were approximately 0.33 mm. A slight variation in the bunch length originated from errors in the quadrupole magnet settings. The estimation of A for each case is as follows: -0.17, -0.20, -0.15, 1.00, and 0.56. According to Eq. (4), this range of A provides a chirp turning range of 9.8 m^{-1}, which is in reasonable agreement with the data in Fig. 3. There are some features of the over-compression in Fig. 3(f) (i.e, cases with the larger magnitude of chirp and smaller bunch length). However, the level of the over-compression in the DEEX beamline is much weaker than in the conventional bunch compressor.

The multipole magnets impart an n-th order correlation to the transverse phase-space (e.g., $\Delta x' \propto x^n$). Thus, a series of multipole magnets would provide or eliminate any correlations that can be approximated by a polynomial series. This concept is adopted by the DEEX beamline to correct the nonlinearity in the initial LPS. Here, the first EEX beamline converts all longitudinal properties to horizontal ones. Multipole magnets in the middle section correct the nonlinear correlation. Then, the second EEX beamline converts the linearized phase-space back to the LPS. The octupole is able to mitigate harmful double-horn features of the bunch, which appear after a strong compression, and often decrease accelerator performance and damages equipment, such as undulators [41]. We demonstrated the proof-of-principle of the nonlinear correction using a single octupole magnet in the DEEX beamline. From this demonstration, the suppression of double-horn features was also observed.

The bunch charge was increased to 700 pC to strengthen the space-charge force at low energy; thus, the third-order correlation in the LPS became more evident. Additionally, the bunch compression was performed such that the higher-order correlations were more evident in the LPS, and they affected the current and energy distributions. For the 700 pC charge, the initial rms bunch length at the DEEX beamline entrance was 0.67 ± 0.03 mm. The DEEX beamline compressed the bunch length to 0.43 ± 0.02 mm, and the current distribution after the compression exhibited a double-horn feature, owing to folded structures that originated from a third-order correlation [see Fig. 4(b)].

Figures 4(a)–(e) show single-shot measurement results of the LPS with different octupole magnet strengths. Figure 4(f) shows the third-order coefficient (a_3) from the polynomial fitting of the measured LPS (see Ref. [42] for further details), and the corresponding rms bunch length. Here, a_3 indicates the strength of the third-order correlation in the LPS distribution. An octupole strength of 182 T/m^3 [Fig. 4(a)] provided a stronger third-order compression. Thus, the outer particles on the head and tail of the beam were pushed further inside, and a_3 decreased from -17.77 m to -45.43 m. Owing to a strengthened third-order compression, the bunch was further compressed, whereas the double-horn feature became stronger compared with the octupole-off case in Fig. 4(b). When the polarity of the octupole-magnet field was flipped, the compression became weaker [Fig. 4(c)]. When the octupole strength was -364 T/m^3 [Fig. 4(d)], a_3 became 2.43 m, which was the smallest magnitude among the presented cases. The phase-space distribution was almost linear in this case, and the double-horn feature disappeared. When the magnitude of the octupole strength was increased further, the LPS distribution exhibited an S-shape [Fig. 4(e)] in the opposite direction to that in Fig. 4(b). The bunch was significantly lengthened, and a_3 further increased.

Outlook and Summary.— We demonstrated DEEX-based longitudinal manipulations, including chirp-less tunable compression, linear time-energy correlation control, and nonlinearity control. More importantly, all these properties can be manipulated simultaneously by a single beamline. These manipulations can enable the optimization of the entire beam's longitudinal properties for a specific application, which may significantly enhance the performance of present accelerators or enable new future accelerators. The DEEX beamline would generate atto-second bunches [21] and impart a large longitudinal chirp for broadband radiation generation [43]. Or, it could be applied to other novel radiation schemes, such as fresh-slice injection [44] and two-color radiation [45]. The recent study of implementing the DEEX beamline to XFEL-Oscillator (XFELO) is another good example supporting the strength of the DEEX method. In Ref. [46], the DEEX beamline was implemented in LCLS-II [47], and it was numerically demonstrated that a bunch compression down to $\sim$ 0.1 ps and an energy spread of $\sim$ 0.001% were feasible, which satisfies XFELO's stringent energy-spread requirements for monochromatic radiations [48, 49].

Because EEX is a developing method of beam manipulation, it introduces various hurdles to overcome such as timing and energy jitter, collective effects, etc. While the challenges particular to our work were overcome, it will be necessary to overcome different challenges for different applications. Despite these future challenges, the results reported here show the potential of the DEEX beamline as a method for achieving arbitrary longitudinal beam manipulations. Further study and development of the DEEX method may reveal a new and powerful way for accelerator scientists to respond to ever challenging demands of modern and future accelerator sciences.

This work was supported by the U.S. Department of Energy, Offices of HEP and BES, under Contract No. DE-AC02-06CH11357, and in part by the National Research Foundation (NRF) of Korea (Grant Nos. NRF-2020R1A2C1010835 and RS-2022-00154676).

---

* gwanghui.ha@gmail.com
† jp@anl.gov
‡ mchung@unist.ac.kr

[1] P. Emma, R. Akre, J. Arthur, R. Bionta, C. Bostedt, J. Bozek, A. Brachmann, P. Bucksbaum, R. Coffee, F.-J. Decker, *et al.*, First lasing and operation of an ångstrom-wavelength free-electron laser, Nature Photonics **4**, 641 (2010).

[2] S. Weathersby, G. Brown, M. Centurion, T. Chase, R. Coffee, J. Corbett, J. Eichner, J. Frisch, A. Fry, M. Gühr, *et al.*, Mega-electron-volt ultrafast electron diffraction at SLAC National Accelerator Laboratory, Review of Scientific Instruments **86**, 073702 (2015).

[3] T. Behnke, J. E. Brau, B. Foster, J. Fuster, M. Harrison, J. M. Paterson, M. Peskin, M. Stanitzki, N. Walker, and H. Yamamoto, The international linear collider technical design report-volume 1: Executive summary, arXiv preprint arXiv:1306.6327 (2013).

[4] S. Huang, Y. Ding, Y. Feng, E. Hemsing, Z. Huang, J. Krzywinski, A. A. Lutman, A. Marinelli, T. J. Maxwell, and D. Zhu, Generating single-spike hard X-ray pulses with nonlinear bunch compression in free-electron lasers, Phys. Rev. Lett. **119**, 154801 (2017).

[5] G. Ha, K.-J. Kim, J. G. Power, Y. Sun, and P. Piot, Bunch shaping in electron linear accelerators, Rev. Mod. Phys. **94**, 025006 (2022).

[6] R. Roussel, G. Andonian, W. Lynn, K. Sanwalka, R. Robles, C. Hansel, A. Deng, G. Lawler, J. B. Rosenzweig, G. Ha, J. Seok, J. G. Power, M. Conde, E. Wisniewski, D. S. Doran, and C. E. Whiteford, Single shot characterization of high transformer ratio wakefields in nonlinear plasma acceleration, Phys. Rev. Lett. **124**, 044802 (2020).

[7] Q. Gao, G. Ha, C. Jing, S. P. Antipov, J. G. Power, M. Conde, W. Gai, H. Chen, J. Shi, E. E. Wisniewski, D. S. Doran, W. Liu, C. E. Whiteford, A. Zholents, P. Piot, and S. S. Baturin, Observation of high transformer ratio of shaped bunch generated by an emittance-exchange beam line, Phys. Rev. Lett. **120**, 114801 (2018).

[8] C. A. Lindstrøm, J. M. Garland, S. Schröder, L. Boulton, G. Boyle, J. Chappell, R. D'Arcy, P. Gonzalez, A. Knetsch, V. Libov, G. Loisch, A. Martinez de la Ossa, P. Niknejadi, K. Põder, L. Schaper, B. Schmidt, B. Sheeran, S. Wesch, J. Wood, and J. Osterhoff, Energy-spread preservation and high efficiency in a plasma-wakefield accelerator, Phys. Rev. Lett. **126**, 014801 (2021).

[9] C. Schroeder, C. Benedetti, S. Bulanov, D. Terzani, E. Esarey, and C. Geddes, Beam dynamics challenges in linear colliders based on laser-plasma accelerators, Journal of Instrumentation **17** (05), P05011.

[10] E. Adli, Towards a PWFA linear col-

lider — opportunities and challenges, Journal of Instrumentation **17** (05), T05006.

[11] C. Jing and G. Ha, Roadmap for structure-based wakefield accelerator (SWFA) r&d and its challenges in beam dynamics, Journal of Instrumentation **17** (05), T05007.

[12] F. Lemery, G. Andonian, S. Doebert, G. Ha, X. Lu, J. Power, and E. Wisniewski, Drive beam sources and longitudinal shaping techniques for beam driven accelerators, Journal of Instrumentation **17** (05), P05036.

[13] B. E. Carlsten and S. J. Russell, Subpicosecond compression of 0.1-1 nc electron bunches with a magnetic chicane at 8 mev, Phys. Rev. E **53**, R2072 (1996).

[14] P. Emma, *X-band RF harmonic compensation for linear bunch compression in the LCLS*, Tech. Rep. LCLS-TN-01-1 (SLAC, Stanford, CA, USA, 2001).

[15] P. Emma, M. Venturini, K. L. F. Bane, G. Stupakov, H.-S. Kang, M. S. Chae, J. Hong, C.-K. Min, H. Yang, T. Ha, W. W. Lee, C. D. Park, S. J. Park, and I. S. Ko, Experimental demonstration of energy-chirp control in relativistic electron bunches using a corrugated pipe, Phys. Rev. Lett. **112**, 034801 (2014).

[16] S. Antipov, S. Baturin, C. Jing, M. Fedurin, A. Kanareykin, C. Swinson, P. Schoessow, W. Gai, and A. Zholents, Experimental demonstration of energy-chirp compensation by a tunable dielectric-based structure, Phys. Rev. Lett. **112**, 114801 (2014).

[17] M. Cornacchia and P. Emma, Transverse to longitudinal emittance exchange, Phys. Rev. Accel. Beams **5**, 084001 (2002).

[18] P. Emma, Z. Huang, K.-J. Kim, and P. Piot, Transverse-to-longitudinal emittance exchange to improve performance of high-gain free-electron lasers, Phys. Rev. Accel. Beams **9**, 100702 (2006).

[19] J. Ruan, A. S. Johnson, A. H. Lumpkin, R. Thurman-Keup, H. Edwards, R. P. Fliller, T. W. Koeth, and Y.-E. Sun, First observation of the exchange of transverse and longitudinal emittances, Phys. Rev. Lett. **106**, 244801 (2011).

[20] E. A. Nanni, W. S. Graves, and D. E. Moncton, Nanomodulated electron beams via electron diffraction and emittance exchange for coherent X-ray generation, Phys. Rev. Accel. Beams **21**, 014401 (2018).

[21] J. Seok, M. Chung, G. Ha, J. G. Power, and M. Conde, Sub-fs electron bunch generation using emittance exchange compressor, in *Proceedings of the 9th International Particle Accelerator Conference*, Vol. 18 (JACOW, 2018) pp. 1501–1503.

[22] P. Piot, Y.-E. Sun, J. G. Power, and M. Rihaoui, Generation of relativistic electron bunches with arbitrary current distribution via transverse-to-longitudinal phase space exchange, Phys. Rev. Accel. Beams **14**, 022801 (2011).

[23] G. Ha, M. Conde, J. Shao, J. Power, and E. Wisniewski, Tunable bunch train generation using emittance exchange beamline with transverse wiggler, in *10th Int. Particle Accelerator Conference (IPAC'19), Melbourne, Australia* (JACOW, 2019) pp. 1612–1614.

[24] Y.-E. Sun, P. Piot, A. Johnson, A. H. Lumpkin, T. J. Maxwell, J. Ruan, and R. Thurman-Keup, Tunable subpicosecond electron-bunch-train generation using a transverse-to-longitudinal phase-space exchange technique, Phys. Rev. Lett. **105**, 234801 (2010).

[25] B. E. Carlsten, K. A. Bishofberger, S. J. Russell, and N. A. Yampolsky, Using an emittance exchanger as a bunch compressor, Phys. Rev. Accel. Beams **14**, 084403 (2011).

[26] G. Ha, J. G. Power, M. Conde, D. S. Doran, and W. Gai, Limiting effects in double EEX beamline, in *Journal of Physics: Conference Series*, Vol. 874 (IOP Publishing, 2017) p. 012061.

[27] G. Ha, J. Power, M. Conde, D. Doran, and W. Gai, Preparations for installation of the double emittance-exchange beamline at the Argonne Wakefield Accelerator facility, in *Proceedings of 38th International Free Electron Laser Conference* (JACOW, 2018) pp. 336–339.

[28] A. Zholents and M. Zolotorev, *A new type of bunch compressor and seeding of a short-wavelength coherent radiation*, Tech. Rep. ANL/APS/LS-327 (Argonne National Lab., Argonne, IL, USA, 2011).

[29] See Supplemental Material of this article for basic principles of the emittance exchange, and transfer matrices of the DEEX beamline (2022).

[30] A. Malyzhenkov and A. Scheinker, Phase space exchange-based bunch compression with reduced CSR effects, arXiv preprint arXiv:1809.05579 (2018).

[31] G. Ha, M. H. Cho, W. Namkung, J. G. Power, D. S. Doran, E. E. Wisniewski, M. Conde, W. Gai, W. Liu, C. Whiteford, Q. Gao, K.-J. Kim, A. Zholents, Y.-E. Sun, C. Jing, and P. Piot, Precision control of the electron longitudinal bunch shape using an emittance-exchange beam line, Phys. Rev. Lett. **118**, 104801 (2017).

[32] G. Ha, M. H. Cho, W. Gai, K.-J. Kim, W. Namkung, and J. G. Power, Perturbation-minimized triangular bunch for high-transformer ratio using a double dogleg emittance exchange beam line, Phys. Rev. Accel. Beams **19**, 121301 (2016).

[33] K.-J. Kim and A. Sessler, Transverse-longitudinal phase-space manipulations and correlations, in *AIP Conference Proceedings*, Vol. 821 (American Institute of Physics, 2006) pp. 115–138.

[34] P. Emma, Z. Huang, K.-J. Kim, and P. Piot, *Transverse-to-longitudinal emittance exchange to improve performance of high-gain free-electron lasers*, Tech. Rep. SLAC-PUB-12038 (SLAC, Stanford, CA, USA, 2006).

[35] M. Conde, S. Antipov, D. Doran, W. Gai, Q. Gao, G. Ha, C. Jing, W. Liu, N. Neveu, J. Power, *et al.*, Research program and recent results at the Argonne Wakefield Accelerator facility (AWA), in *Proceedings of IPAC2017, Copenhagen, Denmark* (JACOW, 2017) pp. 2885–2887.

[36] M. Conde, H. Chen, W. Gai, C. Jing, R. Konecny, W. Liu, D. Mihalcea, P. Piot, J. Power, M. Rihaoui, *et al.*, Commissioning of a 1.3-GHz deflecting cavity for phase-space exchange at the Argonne Wakefield Accelerator, in *Proceedings of IPAC2012, New Orleans, Louisiana, USA* (JACOW, 2012) pp. 3350–3352.

[37] Q. Gao, J. Shi, H. Chen, G. Ha, J. G. Power, M. Conde, and W. Gai, Single-shot wakefield measurement system, Phys. Rev. Accel. Beams **21**, 062801 (2018).

[38] M. G. Minty and F. Zimmermann, *Measurement and control of charged particle beams* (Springer Berlin, Heidelberg, 2003).

[39] D. Xiang and A. Chao, Emittance and phase space exchange for advanced beam manipulation and diagnostics, Phys. Rev. Accel. Beams **14**, 114001 (2011).

[40] See Supplemental Material of this article for the longitudinal chirp after the DEEX beamline (2022).

[41] J. Arthur *et al.*, *Linac Coherent Light Source (LCLS) Conceptual Design Report*, Tech. Rep. SLAC-R593

(SLAC, Stanford, CA, USA, 2002).

[42] See Supplemental Material of this article for the third-order polynomial fitting on longitudinal phase space (2022).

[43] J. Turner, F. Decker, Y. Ding, Z. Huang, R. Iverson, J. Krzywinski, H. Loos, A. Marinelli, T. Maxwell, H. Nuhn, *et al.*, FEL over-compression in the LCLS, in *Proceedings of the 36th International Free Electron Laser Conference Basel, Switzerland* (JACOW, 2014).

[44] A. A. Lutman, T. J. Maxwell, J. P. MacArthur, M. W. Guetg, N. Berrah, R. N. Coffee, Y. Ding, Z. Huang, A. Marinelli, S. Moeller, *et al.*, Fresh-slice multicolour X-ray free-electron lasers, Nature Photonics **10**, 745 (2016).

[45] A. A. Lutman, R. Coffee, Y. Ding, Z. Huang, J. Krzywinski, T. Maxwell, M. Messerschmidt, and H.-D. Nuhn, Experimental demonstration of femtosecond two-color X-ray free-electron lasers, Phys. Rev. Lett. **110**, 134801 (2013).

[46] J. Seok, G. Ha, J. Power, M. Conde, and M. Chung, Suppression of correlated energy spread using emittance exchange, in *10th International Particle Accelerator Conference (IPAC'19), Melbourne, Australia* (JACOW, 2019) pp. 3275–3278.

[47] J. Stohr, *Linac Coherent Light Source II (LCLS-II) Conceptual Design Report*, Tech. Rep. LCLSII-1.1-DR-0001-R0 (SLAC, Stanford, CA, USA, 2011).

[48] K.-J. Kim, Y. Shvyd'ko, and S. Reiche, A proposal for an X-ray free-electron laser oscillator with an energy-recovery linac, Phys. Rev. Lett. **100**, 244802 (2008).

[49] W. Qin *et al.*, Start-to-end simulations for an X-ray FEL oscillator at the LCLS-II and LCLS-II-HE, in *Proc. of International Free Electron Laser Conference (FEL'17), Santa Fe, NM, USA* (JACOW, 2018) pp. 247–250.